Regular Article

Functionalization of the Single-walled Carbon Nanotubes by Sulfur Dioxide and Electric Field Effect, a Theoretical Study on the Mechanism

S. Peymani, M. Izadyar* and A. Nakhaeipour

Department of Chemistry, Faculty of Sciences, Ferdowsi University of Mashhad, Mashhad, Iran

(Received 18 February 2016, Accepted 16 June 2016)

In this study, kinetics and mechanism of the sulfur dioxide adsorption on the single-walled carbon nanotubes (CNT) are investigated. Three single-walled carbon nanotubes, including the armchair (6,6), chiral (6,5) and zigzag (6,0) CNTs were chosen as the models and the different orientations of SO_2 molecule relative to the CNT axis were considered. The B3LYP functional within the 6-31G(d) basis set was used for the theoretical calculations. For all orientations, reaction Gibbs free energies ($\Delta G°$) were calculated and the transition state structures were investigated for the spontaneous reactions. Chiral single-walled carbon nanotube (6,5) showed the least activation energy (11.72 kcal mol^{-1}) while the armchair model showed the highest one (17.93 kcal mol^{-1}). Natural bond orbital analysis showed that the electronic charge is transferred from CNT to sulfur dioxide. Topological analysis confirmed the C-S bond formation at the transition state. Density of states analysis showed that Fermi level energy is increased in armchair model. The application of the external electric field indicated that the CNTs stability and the functionalization energies are improved. Based on the obtained data, by using the electric field, it is possible to elevate the conductivity of CNT and the functionalization rate of SWCNT for industrial applications.

Keywords: Nanotube, Sulfur dioxide, Electric field effect, Functionalization

INTRODUCTION

Since their discovery by Iijima in 1991 [1], carbon nanotubes have been of great interest. These nanomaterials have unique properties such as high thermal conductivity, high surface area and remarkable ratio of their surface to volume [2,3]. Due to the surface atoms, an environmental small change causes a large change in the electrical properties of CNTs [4].

Moreover, CNTs have high potential in various areas including electronics [5,6], nanomedicine [7,8], composite materials [9,10], biomedicine [11], nanoelectromechanical systems [12], field-effect transistors [13,4], separation sciences [14], sensors and actuators [15]. However, this huge potential can redound to effective usages if CNTs are functionalized by different groups. The functionalization methods of CNTs are summarized into two categories

*Corresponding author. E-mail: izadyar@um.ac.ir

including the covalent and non-covalent linkages.

Covalent functionalization is based on the formation of a covalent bond between the functional groups and carbon skeleton of CNT through the direct and indirect reactions. Also non-covalent modifications can be classified into two groups of endohedral filling and non-covalent surface interactions [16].

There are many reports in the literature on the functionalization of CNTs. For example, CNTs have been functionalized by nitrosoalkenes (NAS) and thionitroso-alkenes (TNAS) [17], $Cr(CO_3)$ [18], acetone [19], aniline [20], carboxyl group [21], NH_2 and $CONH_2$ groups [22], polymers [23], benzene [24], phenol [25], alkylpolyglycerol derivatives [26], thiophen [27], dimethyl phthalate [28], NO_2, CO_2, O_2 [29], N_2, CH_4, NH_3, H_2, Ar [30], thymine and uracil [31] for various applications.

Zhang _et al_. reported the sensing properties of Pt-(8,0) CNT to some gaseous molecules such as SO_2 and concluded that Pt-SWCNT is highly sensitive to SO_2 [32].

Pabitra *et al*. studied the sensitivity of Ge-CNT against the gaseous molecules such as SO_2 by *ab initio* methods [33]. They found that the S atom interacts with C atoms in a distance of 1.829 Å, in accordance to the C-S bond. A cleavage in the density of states (DOS) spectra was interpreted by the SO_2 strong adsorption and finally concluded that (6,0) Ge-CNT has a high potential for SO_2 detection.

Nagar *et al*. investigated the adsorption of SO_2 molecule using the doped (8,0) CNT with Si [29]. They found that before Si doping, SO_2 is physically adsorbed on the CNT from the S end in a distance of 2.3 Å with an adsorption energy of -0.24 eV and charge transfer value of 0.08e, while after doping the C-S bond length, adsorption energy and charge transfer values changed to 1.6 Å, -2.58 eV and 0.45e, respectively. These changes indicated a chemical bond formation and increase in the conductivity of nanotube.

SWCNT is known as a chemical sensor for the detection of the gaseous molecules such as SO_2. Although the experimental studies have been performed on the adsorption of SO_2 on SWCNTs, based on our knowledge, the mechanism and kinetics of this reaction is still unknown [34,35].

Applying the electric field is an effective method for the correction of low dimension. For example, Peter and his colleagues showed that one H_2 molecule can automatically be separated and adsorbed on the N-doped graphene in the presence of an electric field [36]. The dissociative adsorption energy barrier of an H_2 molecule on a pure graphene layer reduced from 2.7 eV to 2.5 eV on the N-doped graphene and to 0.88 eV on the N-doped graphene under the electric field of 0.005 (a.u.), and when a high electric field of 0.01 a.u. was applied, the reaction barrier disappeared.

Sun and coworkers demonstrated that an electric field can improve the hydrogen storage capacity on the BN layers [37]. Alfieri and coworkers found an interesting phenomenon in which the energy gap of SiCNT can be considerably manipulated by applying a transverse electric field [38]. In addition, Zhang et al. studied the effect of the electric field on the adsorption of SO_2 molecule on (5,5) SiCNT [39]. They found that SO_2 can be chemically adsorbed on the Si-C bonds under the electric field within a reduction in the energy gap.

There is a problem in the past thermodynamic studies that tried to problem opening from the view of simplifying the bond forming of sulfur with surface, however, recent studies of our research group on SO_2 in the gas phase indicate that the formation of the heterocyclic compounds proceeds through a cheletropic reaction [40]. Therefore, this research intends to look at this problem from the mechanism viewpoint, using the quantum chemistry methods. In this study, different adsorption sites on SWCNTs, the nature of interactions, electric field effect on the adsorption and some probable correlations between the reactivity indices and activation energy are analyzed and discussed.

COMPUTATIONAL DETAILS

In this study, the interaction of sulfur dioxide and SWCNT, including (6,6), (6,5) and (6,0) models (Figs. S1-S3), is investigated in the gas phase. Different situations, inside, outside and nanotubes edges, were considered by using the density functional theory (DFT) method, B3LYP hybrid functional and 6-31G(d) basis set. All calculations were performed with the Gaussian 09 software [41]. SWCNT functionalization reaction by sulfur dioxide is shown in Eq. (1).

$$SWCNT\text{-}H_2 + SO_{2\,(g)} \longrightarrow SWCNT\text{-}SO_2 + H_{2\,(g)} + Energy \tag{1}$$
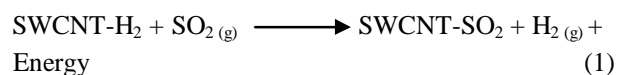
In this equation, carbon atoms on the edges are H-capped. Gaussview 05 [42] and nanotube modeler [43] softwares were used for drawing the structures. The effect of different orientations of the SO_2 molecule on the nanotube external surface was also considered during the adsorption process (Fig. 1). Figure 1, A shows the parallel situation of SO_2 relative to the SWCNT axis. B and C show the vertical orientation of SO_2 through the S and O atoms, respectively. In the case of D, however, there is a specific orientation through which only one oxygen atom can properly interact with SWCNT.

In all cases, harmonic vibrational frequency calculations were carried out to verify the nature of the stationary points along the reaction. The absorption energies were obtained according to Eq. (2),
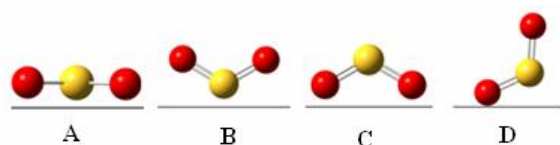
Fig. 1. Different orientations of sulfur dioxide molecule relative to the carbon nanotubes axis.

$$\Delta E_{ads} = E_{SO2@nanotube} - (E_{nanotube} + E_{SO2}) \qquad (2)$$

where, $E_{SO2@nanotube}$ is the energy of functionalized nanotube and $E_{nanotube}$ and E_{SO2} are the isolated nanotube and SO_2 energies, respectively.

To gain insight into the reaction mechanism and activation energy, synchronous-transit guided of quasi-Newton (STQN) method is applied. The obtained structures of the transition states (TSs) are examined by intrinsic reaction coordinate (IRC) method and the corresponding one imaginary vibrational frequency. Since the global electron density transfer (GEDT) is a key factor in the TS energetic, quantum theory of atoms in molecules (QTAM) is used. The stability of the TS is investigated by the natural bond orbital (NBO) method. Quantum reactivity indices, including the electronic chemical hardness (η), electronic chemical potential (μ_e), electrophilicity (ω) and charge transfer (ΔN), are calculated according to the Koopmans method [44]. Finally, the effect of electric field on the adsorption process is studied. To do so, the reactants, transition state structures and products are exposed to the electric field strength of 0.001 a.u., equivalent to a field of 1.2 Tesla, at the B3LYP/6-31G(d) level of theory. Then, calculated ΔE and $\Delta E^{\neq}$, as the single point energy changes of the reaction and activation, respectively, are analyzed.

RESULTS AND DISCUSSION

After optimizing the structures, the absorption energies of SO_2 molecules on the SWCNTs, for the structures of **a-f**, are reported in Table 1. Figures 2 and 3 show the final optimized structures of the products inside and at the edge of CNT, respectively. Based on the results, the maximum energy of adsorption is related to **d** structure.

Thermodynamic and Kinetic Parameters

Thermodynamic parameters for the functionalization of SWCNTs at the edge site are calculated and reported in Table 2. It should be noted that in other situations, the calculated Gibbs free energies are positive ($\Delta G > 0$), therefore, they are excluded in the next steps of kinetic studies.

According to this table, all reactions are spontaneous, exothermic and functionalization by chiral SWCNT is more favorable than other models, thermodynamically.

For investigation of the kinetic aspects of this functionalization and awareness of the nature of transition states, STQN procedure is applied [45]. Figure 4 shows the optimized structures of the obtained TSs for the three models.

Calculated imaginary vibrational frequencies of the TSs for (6,6), (6,5) and (6,0) SWCNTs, are 284.7, 262.9 and 103.5 i cm^{-1}, respectively, indicating a first-order saddle point on the reaction coordinate.

Geometric parameters of the transition states are given in Tables S1 to S3. According to these tables, fundamental geometrical changes concern to the C-S bonds. Mean value of 1.8 Å for the C-S bond length in the products shows its covalence nature. Comparing the bond length changes during the functionalization shows that C-S bond formation could be a driving force for the reaction. Activation and kinetic parameters are calculated and reported in Table 3.

Based on the activation energies, the functionalization of the chiral SWCNT is faster than that of other models, by an energy difference of about 6.0 kcal mol^{-1}. Theoretical trend in the rate of the functionalization reaction is in accordance with: (6,5) > (6,0) > (6,6).

Negative activation entropy shows that five-member ring formation at the SWCNT edge reduces the degrees of freedom at the TS in line with the cycloaddition reactions. The reaction progress is shown by the potential energy diagram in Fig. 5. As indicated in this figure, all of the studied reactions are spontaneous and chiral SWCNT has the least activation Gibbs free energy.

Table 1. Calculated Adsorption Energies (kcal mol^{-1}) of SO$_2$ on the SWCNTs for the Structures of **a-f**

	a[a]	b	c	d	e	f
(6,6)CNT	-2.5	30.1	30.1	-2.4	65.6	-1.8
(6,5)CNT	-1.9	52.2	68.9	-3.1	68.9	-2.8
(6,0)CNT	3.4	-1.9	3.4	-10.9	-1.7	15.3

[a]**a-f** structures are show in Fig. S4.
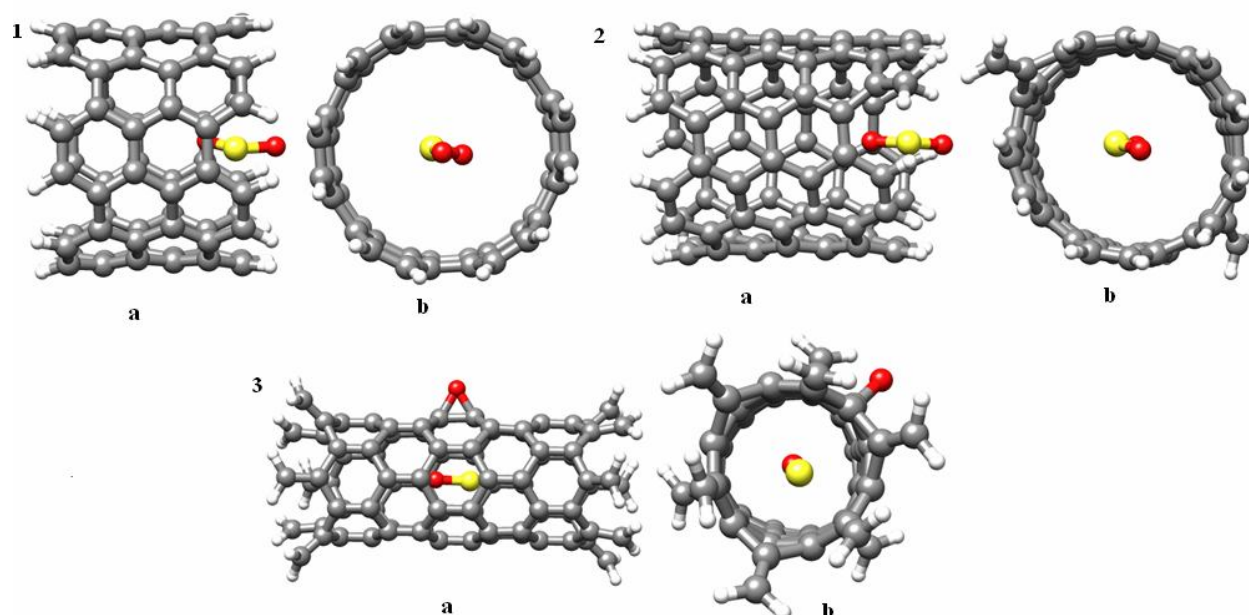
Fig. 2. Optimized functionalized nanotubes from the inside by using B3LYP/6-31G(d), 1) (6,6) CNT, 2) (6,5) CNT, 3) (6,0) CNT, (a) side view, (b) front view.

NBO ANALYSIS

NBO analysis is carried out to determine the donor-acceptor interactions during the functionalization process by using the second-order perturbation stabilization energies, E(2). The most important interactions at the TSs are reported in Table 4. As seen in this table, the sum of lone pair (Lp) interactions at the TS (6,6), TS (6,5) and TS (6,0) are 81.4, 115.4 and 90.0 kcal mol^{-1}, respectively.

E(2) values of the reactants indicate the resonance effects of the aromatic rings around the reaction center. The corresponding E(2) values at the TS indicate the effective electron transfer at the TS and the proper interaction of sulfur, oxygen and carbon atoms. Based on the NBO analysis and the obtained activation energy data of all studied models, a linear correlation between the activation energy and the sum of the stabilization energies at the TSs is proposed and shown in Fig. 6.

QTAIM ANALYSIS

To obtain some information on the nature of the C-S

Table 3. Thermodynamic Parameters for the Functionalization of SWCNT at the Edge Site

CNT	(6,6)	(6,5)	(6,0)
ΔG (kcal mol^{-1})	-80.1	-85.6	-17.4
ΔH (kcal mol^{-1})	-93.8	-100.5	-29.2
ΔS (cal mol^{-1} K^{-1})	-45.9	-49.9	-39.6
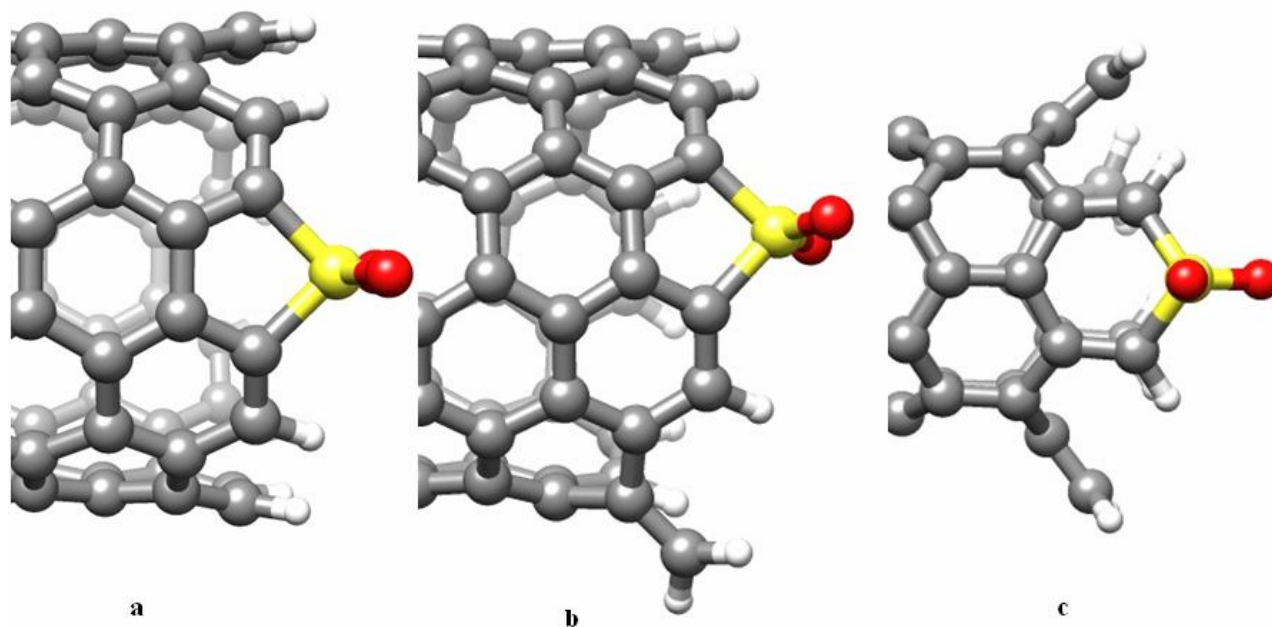
Fig. 3. Optimized structures of the functionalized SWCNT by SO_2 at the edge (a) (6,6) CNT, (b) (6,5) CNT, (c) (6,0) CNT.

Table 3. Kinetic Parameters of the Functionalization Reaction of SWCNTs at 298 K

Parameter	CNT (6,6)	CNT (6,5)	CNT (6,0)
$\Delta G^{\neq}$ (kcal mol^{-1})	30.8	25.6	29.9
$\Delta H^{\neq}$ (kcal mol^{-1})	16.7	10.5	15.8
$\Delta S^{\neq}$ (cal mol^{-1} K^{-1})	-47.2	-50.6	-47.4
Ea (kcal mol^{-1})	17.9	11.7	17.0
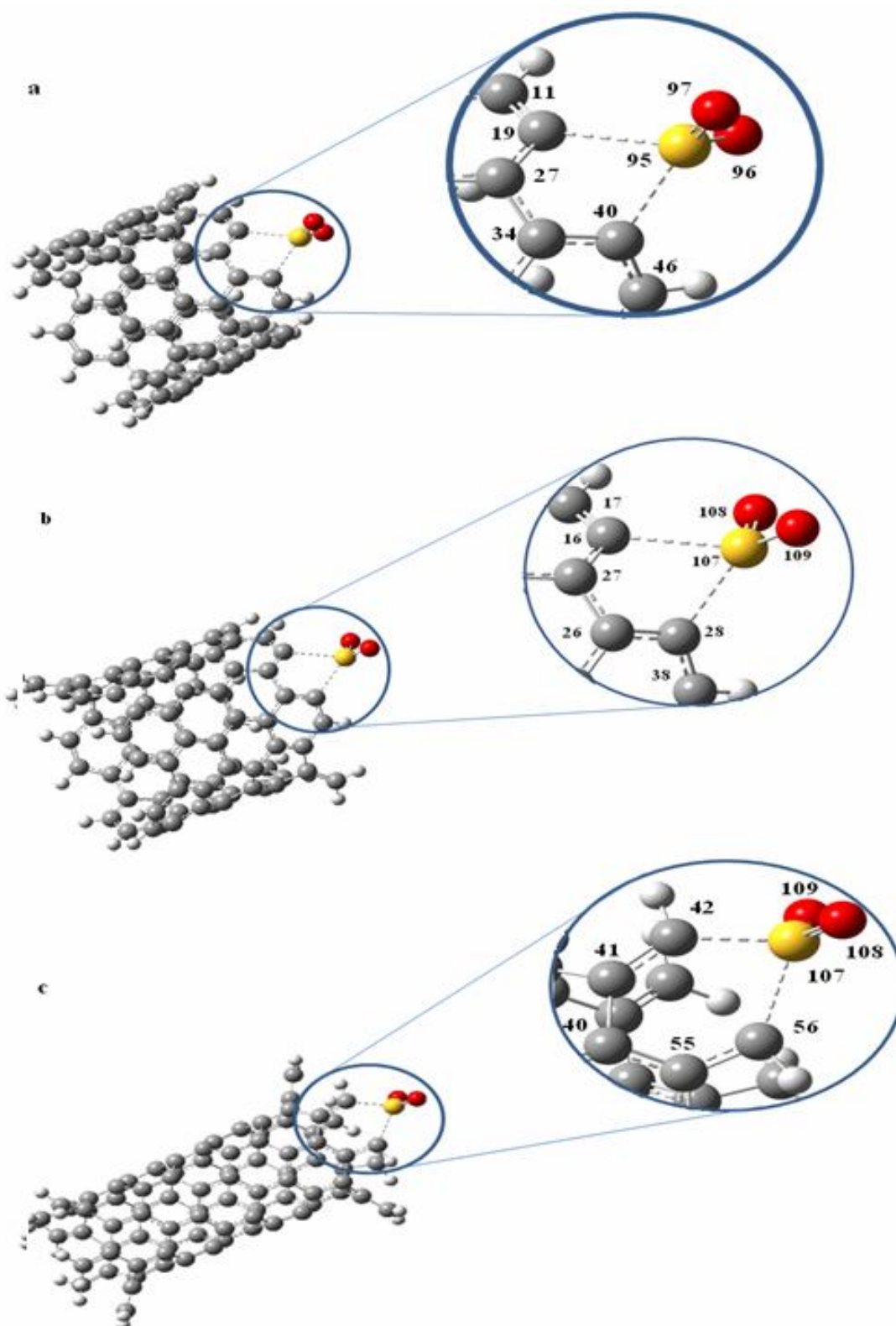
Fig. 4. Optimized structures of the TSs, (a) (6,6) CNT, (b) (6,5) CNT, (c) (6,0) CNT.
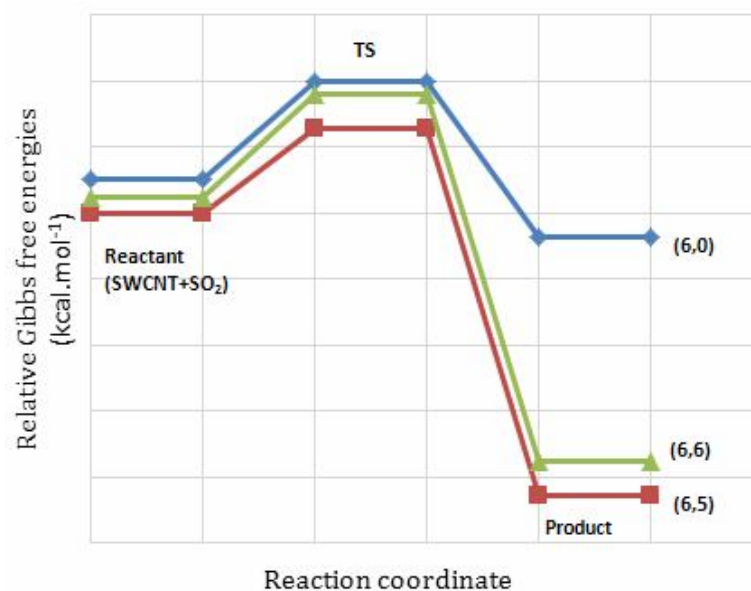
Fig. 5. Potential energy diagram of the SWCNT functionalization reaction by sulfur dioxide.
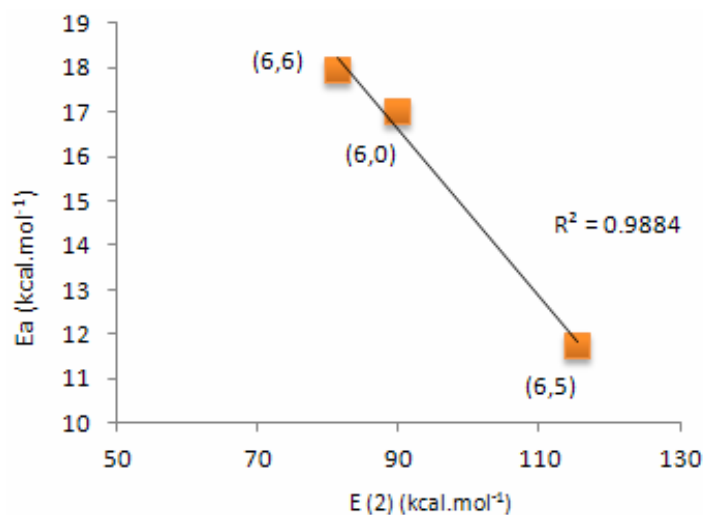
Fig. 6. Linear correlation between the activation energy and sum of the stabilization energy at the TSs.

bond formation between the carbon nanotubes and sulfur dioxide, topological parameters such as electron density, $\rho(r)$, Laplacian, $\nabla^2\rho(r)$, Hamiltonian of the electron density, $H(r)$, potential energy density, $V(r)$ and kinetic energy density, $G(r)$ are calculated and reported in Table 5.

The growth of electron density of the C-S bond at the TSs relative to the reactant shows the bond order enhancement during the functionalization reaction. Different signs of $\nabla^2\rho(r)$ for the C-S bonds show different extents of bond formation at the TSs. Absolute values of the potential energy density to the kinetic energy density ratios are greater than one indicating the creation of a middle

Table 4. Important Natural Bond Orbital Interactions of the Reactants and TSs in Three Models and Their Second-Order Perturbation Stabilization Energies, E(2) in kcal mol^{-1}

	Reactant	E(2)	TS	E(2)
	$\pi_{C11-C19} \rightarrow \pi^*_{C5-C12}$	19.6	$\pi_{C11-C19} \rightarrow \pi^*_{C5-C12}$	41.9
	$\pi_{C11-C19} \rightarrow \pi^*_{C20-C27}$	17.4	$\pi_{C34-C41} \rightarrow \pi^*_{C28-C35}$	16.6
(6,6) CNT@	$\pi_{C20-C27} \rightarrow \pi^*_{C21-C28}$	17.7	$\pi_{C34-C41} \rightarrow \pi^*_{C40-C46}$	13.5
SO$_2$	$\pi_{C35-C42} \rightarrow \pi^*_{C41-C47}$	15.5	$\pi_{C34-C41} \rightarrow \pi^*_{C47-C52}$	21.6
			$\pi_{C40-C46} \rightarrow \pi^*_{C47-C52}$	14.9
			$Lp_{S95} \rightarrow \sigma^*_{C19-S95}$	29.8
			$Lp_{S95} \rightarrow \sigma^*_{C40-S95}$	34.8
			$Lp_{O97} \rightarrow \sigma^*_{C40-S95}$	16.8
	$\pi_{C14-C25} \rightarrow \pi^*_{C15-C17}$	19.2		
	$\pi_{C14-C25} \rightarrow \pi^*_{C16-C27}$	15.4	$Lp_{S107} \rightarrow \sigma^*_{C28-S107}$	12.7
(6,5) CNT@	$\pi_{C16-C27} \rightarrow \pi^*_{C15-C17}$	16.5	$Lp_{O108} \rightarrow \sigma^*_{C28-S107}$	54.3
SO$_2$	$\pi_{C16-C27} \rightarrow \pi^*_{C26-C28}$	16.9	$Lp_{O109} \rightarrow \sigma^*_{C28-S107}$	32.9
	$\pi_{C26-C28} \rightarrow \pi^*_{C34-C36}$	17.2	$Lp_{O109} \rightarrow \sigma^*_{C28-S107}$	15.5
	$\pi_{C26-C28} \rightarrow \pi^*_{C37-C38}$	20.0		
	$\pi_{C34-C36} \rightarrow \pi^*_{C35-C45}$	20.4		
	$\pi_{C24-C26} \rightarrow \pi^*_{C23-C25}$	15.0	$\pi_{C24-C26} \rightarrow \pi^*_{C37-C49}$	13.4
	$\pi_{C24-C26} \rightarrow \pi^*_{C38-C39}$	13.3	$\pi_{C24-C26} \rightarrow \pi^*_{C41-C42}$	14.6
(6,0) CNT@	$\pi_{C38-C39} \rightarrow \pi^*_{C36-C37}$	16.8	$\pi_{C38-C40} \rightarrow \pi^*_{C37-C39}$	17.0
SO$_2$	$\pi_{C40-C55} \rightarrow \pi^*_{C38-C39}$	11.8	$\pi_{C38-C40} \rightarrow \pi^*_{C54-C55}$	19.9
	$\pi_{C40-C55} \rightarrow \pi^*_{C41-C42}$	19.1	$\pi_{C41-C42} \rightarrow \pi^*_{C24-C26}$	12.2
	$\pi_{C41-C42} \rightarrow \pi^*_{C24-C26}$	18.9	$\pi_{C54-C55} \rightarrow \pi^*_{C38-C40}$	19.32
	$\pi_{C41-C42} \rightarrow \pi^*_{C40-C55}$	13.4	$Lp_{O108} \rightarrow \sigma^*_{C42-S107}$	21.0
			$Lp_{O108} \rightarrow \sigma^*_{C56-S107}$	23.5
			$Lp_{O109} \rightarrow \sigma^*_{C42-S107}$	15.7
			$Lp_{O109} \rightarrow \sigma^*_{C56-S107}$	30.2

covalent bond at the transition states. Negative low values of H(r), at the transition states, show that the interactions are mainly potential in nature.

ELECTRIC FIELD EFFECTS

The effect of the electric field (EF) is investigated on the kinetics of these reactions and the obtained results in the presence and absence of an electric field are compared in Table 6.

As show in this table, the adsorption energy of SO$_2$ on SWCNT increases in the presence of electric field, in contrast to the activation energy behavior. Zigzag SWCNT shows the most sensitivity to the electric field by a value of

Table 5. Topological Parameters at the TSs (a.u.) Calculated at the B3LYP/6-31G(d) Level of Theory

	(6,0) C42- S107	(6,5) C16- S107	(6,6) C19- S95
	(6,0) C56- S107	(6,5) C28- S107	(6,6) C40- S95
$\rho(r)$	0.04	0.28	0.12
	0.07	0.07	0.07
	-0.05	-0.97	-0.07
$\nabla^2\rho(r)$	0.04	0.04	0.01
H	-0.001	-0.04	-0.05
	-0.01	-0.01	-0.02
-V/G	1.14	1.18	2.65
	1.62	1.59	1.87

Table 6. Calculated Single Point Energies (kcal mol^{-1}) in the Electric Field (EF) of 0.001 a.u. at the B3LYP/6-31G(d) Level

CNT		(6,6)	(6,5)	(6,0)
ΔE	without EF	-98.3	-104.9	-30.4
	in EF	-100.5	-105.7	-32.9
$\Delta E^{\neq}$	without EF	16.8	10.6	15.9
	in EF	13.6	8.5	13.7

2.47 kcal mol^{-1}, while the chiral type is less sensitive.

Accordingly, the rate of the functionalization is not only increased in the presence of an external electric field, but also the reaction is more favorable from the thermodynamic viewpoint. Since the electric field perturbs the molecular properties of the studied systems, its effect on the quantum reactivity indices is investigated and reported in Table 7.

Based on the data reported in this table, electric field reduces the electronic chemical potential of the TS which stabilizes it. An opposite behavior is seen for the reactants which means an increase in their chemical reactivity.

Generally, if the dipole moment of a structure is large, the corresponding dipole-dipole interaction with the surrounding will be increased. The electric field causes an increase in the dipole moment and therefore increases dipole-dipole interactions. Therefore, if the functionalization reaction occurs in a polar solvent, an increment in the rate of reaction is expected.

Investigation of the changes in the electrophilicity index in the presence of the electric field shows no regular rule. To analyze the possible correlation between the activation energy and quantum reactivity indices, correlation graphs are plotted and correlation coefficients are calculated. Linear regression coefficients of the activation energy as a function of ω, η, μ_e were 0.7, 0.9 and 0.4, respectively, indicating a good correlation of the activation energy and chemical hardness, in accordance with the previous results [41].

Table 7. Calculated Quantum Reactivity Indices (kcal mol^{-1}, µ in Debye) in the Presence and Absence of the Electric Field

	μ_e		η		ω		μ	
	FA[a]	FP[b]	FA	FP	FA	FP	FA	FP
(6,6) Reactant	-87.31	-86.73	28.41	29.30	134.17	128.34	4.60	3.48
(6,6) TS	-95.97	-96.13	12.31	12.02	374.05	384.29	11.09	14.09
(6,6) Product	-85.66	-85.37	38.16	37.79	96.13	96.44	7.68	9.31
(6,5) Reactant	-89.37	-89.40	22.50	22.79	177.47	175.86	7.19	9.74
(6,5) TS	-93.82	-93.97	13.12	13.12	355.29	336.51	12.99	17.10
(6,5) Product	-89.74	-89.51	27.13	27.02	148.40	148.27	8.27	11.40
(6,0) Reactant	-94.85	-94.57	19.44	19.57	231.38	228.47	2.26	7.76
(6,0) TS	-100.40	-99.69	22.82	23.08	220.88	215.28	11.03	17.06
(6,0) Product	-103.09	-102.86	18.32	18.12	290.10	292.03	12.97	18.88

[a]Field absence. [b]Field presence.

CONCLUSIONS

The adsorption of sulfur dioxide molecule on the (6,6), (6,5) and (6,0) single-walled carbon nanotubes was theoretically studied. For doing so, B3LYP theoretical level and 6-31G(d) basis set were applied and the following results were obtained.

Sulfur dioxide adsorption on the inner and outer walls of the SWCNTs models takes place physically, while on the nanotube edges shows a chemical nature.

-Analysis of the geometrical parameters during the reactions indicated that the C-S bond formation could be a driving force for the reaction.

-The use of an electric field, stabilizes the TS structures and increases the reaction rates, theoretically, which can be interpreted by dipole-dipole interactions, especially in the solvents. Also, the quantum reactivity indices such as electronic chemical potential and chemical hardness are affected by the electric field.

- NBO analysis showed that main stabilizing interactions at the TSs are related to $Lp_S \rightarrow \sigma^*_{C-S}$.

- QTAIM analysis confirmed a covalent nature of the forming C-S bond at the TS, according to the adsorption energies at the SWCNT edges.

ACKNOWLEDGEMENTS

REFERENCES

[1] Iijima, S., Helical microtubules of graphitic carbon. *Nature*. **1991**, *354*, 56-58, DOI: 10.1038/354056a0.

[2] Bega, S.; Rizwana, M.; Sheikhb, A. M.; Saquib Hasnaina, M.; Anwerc, K.; Kohlia, K, Advancement in carbon nanotubes: basics, biomedical applications and toxicity. *J. Pharm. Pharmacol*. **2011**, *63*, 141-

163, DOI: 10.1111/j.2042-7158.2010.01167.x.

[3] Che, J.; Çagin, T.; Goddard, W. A., Thermal conductivity of carbon nanotubes. *Nanotechnology*. **2000**, *11*, 65-69, DOI: 10.1088/0957-4484/11/2/305.

[4] Liu, S.; Shen, Q.; Cao, Y.; Gan, L.; Wang, Z. H.; Steigerwald, M. L.; Guo, X., Chemical functionalization of single-walled carbon nanotube field-effect transistors as switches and sensors. *Coord. Chem. Rev*. **2010***, 254*, 1101-1116, DOI: 10.1016/ j.ccr.2009.11.007.

[5] Ng, S. H.; Wang, J.; Guo, Z. P.; Chen, J.; Wang, G. X.; Liu, H. K., Single wall carbon nanotube paper as anode for lithium-ion battery. *Electrochim. Acta*. **2005**, *51*, 23-28, DOI: 10.1016/ j.electacta.2005.04.045.

[6] Chien. Y. M.; Lefevre. F.; Shih. I.; Izquierdo. R., A solution processed top emission OLED with transparent carbon nanotube electrodes. *Nanotechnology*, **2010**, *21*, 1-5, DOI: 10.1088/0957-4484/21/13/134020.

[7] Pantarotto, D.; Singh, R.; McCarthy, D.; Erhardt, M.; Briand, J. P.; Prato, M.; Ostarelos, K.; Bianco, A, Functionalized carbon nanotubes for plasmid DNA gene delivery. *Ang. Chem. Int. Ed.* **2004**, *43*, 5242-5246, DOI: 10.1002/anie.200460437.

[8] Klumpp, C.; Kostarelos. K.; Prato. M.; Bianco. A. Functionalized carbon nanotubes as emerging nanovectors for the delivery of therapeutics. *Biochim. Biophys. Acta: Biomembranes*. **2006**, *1758*, 404-412, DOI: 10.1016/j.bbamem.2005.10.008.

[9] Bauhofer, W.; Kovacs, J. Z., A review and analysis of electrical percolation in carbon nanotube polymer composites. *Compos. Sci. Technol*. **2009**, *69*, 1486-1498, DOI: 10.15480/882.392.

[10] Chou, T. W.; Gao, L. M.; Thostenson, E. T.; Zhang, Z. G.; Byun, J. -H., (2010) An assessment of the science and technology of carbon nanotube fibers and composites. *Compos. Sci. Technol*. **2010**, *70*, 1-19, DOI: 10.1016/j.compscitech.2009.10.004.

[11] He, H.; Pham-Huy, L. A.; Dramou, P.; Xiao, D.; Zuo, P.; Pham-Huy, C., Carbon nanotubes: applications in pharmacy and medicine. *BioMed Res. Int*. 2013, 1-13. DOI: 10.1155/2013/578290.

[12] Ganzhorn, M.; Klyatskaya, S.; Ruben, M.;

Wernsdorfer, W., Carbon nanotube nanoelectro-mechanical systems as magnetometers for single-molecule magnets. *ACS Nano*. **2013***, 7*, 6225-6236, DOI: 10.1021/nn402968k.

[13] Kauffman, D. R.; Star, A., Electronically monitoring biological interactions with carbon nanotube field-effect transistors. *Chem. Soc. Rev*. **2008**, *37*, 1197-1206, DOI: 10.1039/b709567h

[14] Herrera-Herrera, A. V.; Gonzalez-Curbelo, M. A.; Hernandez-Borges, J.; Rodriguez-Delgado, M. A., Carbon nanotubes applications in separation science: A review. *Anal. Chim. Acta*. **2012**, *734*, 1-30, DOI: 10.1016/j.aca.2012.04.035.

[15] Schnorr, J. M.; Swager, T. M., Emerging applications of carbon nanotubes. *Chem. Mater*. **2011**, *23*, 646-657, DOI**:** 10.1021/cm102406h.

[16] Ren, F.; Yu, H.; Wang, L.; Saleem, M.; Tian, Z.; Ren, P., Current progress on the modification of carbon nanotubes and their application in electromagnetic wave absorption. *RSC Adv*. **2014**, *4*, 14419-14431, DOI: 10.1039/C3RA46989A.

[17] Pankhao, D.; Morakot, N.; Keawwangchai, S.; Wanno, B, Theoretical investigation of hetero-diels-alder functionalizations on swcnt and their reaction properties. *Int. Trans. J. Eng. Manag. Sci. Tech.* **2013**, *4*, 145-156, http://TuEngr.com/V04/145-156.pdf

[18] Nunzi, F.; Sgamellotti, A.; Angelis, F. D, Cr(CO)$_3$-Activated diels-alder reaction on single-wall carbon nanotubes: A DFT investigation. *J. Chem. Eur.* **2009**, *15*, 4182-4189, DOI: 10.1002/chem.200802440.

[19] Kazachkin, D.; Nishimura, Y.; Irle, S.; Morokuma, K.; Vidic, R. D.; Borguet, E., Interaction of Acetone with single wall carbon nanotubes at cryogenic temperatures: a combined temperature programmed desorption and theoretical study. *Langmuir*. **2008**, *24*, 7848-7856, DOI: 10.1021/la800030y.

[20] Peles-Lemli, B.; Matisz, G.; Kelterer, A. -M.; Fabian, W. M. F.; Kunsági-Máté, S., Noncovalent interaction between aniline and carbon nanotubes: effect of nanotube diameter and the hydrogen-bonded solvent methanol on the adsorption energy and the photophysics. *J. Phys. Chem. C*. **2010**, *114*, 5898-5905, DOI: 10.1021/jp908505q.

[21] Kar, T.; Akdim, B.; Duan, X.; Pachter, R., Open-

ended modified single-wall carbon nanotubes: a theoretical study of the effects of purification. *Chem. Phys. Lett.* **2006**, *423*, 126-130, DOI: 10.1016/j.cplett.2006.02.089.

[22] Veloso, M. V.; Filho, A. G. S.; Filho, J. M.; Fagan, S. B.; Mota, R., *Ab initio* study of covalently functionalized carbon nanotubes. *Chem. Phys. Lett.* **2006**, *430*, 71-74. DOI: 10.1016/j.cplett.2006.08.082.

[23] Alturaif, H. A.; Alothman, Z. A.; Shapter, J. G.; Wabaidur, S. M., Use of carbon nanotubes (CNTs) with polymers in solar cells. *Molecules*. **2014**, *19*, 17329-17344, DOI: 10.3390/molecules191117329.

[24] Kanga, H.; Limb, S.; Parkb, N.; Chunc, K. -Y.; Baik, S., Improving the sensitivity of carbon nanotube sensors by benzene functionalization. *J. Sens. Act. B.* **2010**, *147*, 316-321, DOI: 10.1016/j.snb.2010.03.028.

[25] Peyghan, A. A.; Baei, M. T.; Moghimi, M.; Hashemian, S., Phenol adsorption study on pristine, Ga-, and In-doped (4,4) armchair single-walled boron nitride nanotubes. *Comput. Theor. Chem.* **2012**, *997*, 63-69, DOI: 10.1016/j.comptc.2012.07.037.

[26] Setaro, C.; Popeney, C. S.; Trappmann, B.; Haag, R.; Reich, S., Interaction between single-walled carbon nanotubes and alkylpolyglycerol derivatives. *Phys. Status Solidi B*. **2010**, *247*, 11-12, 2758-2761, DOI: 10.1002/pssb.201000829.

[27] Goering, J.; Burghaus, U., Adsorption kinetics of thiophene on single-walled carbon nanotubes (CNTs). *Chem. Phys. Lette*. **2007**, *447*, 121-126, DOI: 10.1002/pssb.201000829.

[28] Wang, J.; Wang, F.; Yao, J.; Wang, R.; Yuan, H., Masakorala, K.; Choi, M. M. F., Adsorption and desorption of dimethyl phthalate on carbon nanotubes in aqueous copper(II) solution. *Colloids Surf. A*. **2013**, *417*, 47-56, DOI: 10.1016/j.colsurfa.2012.10.058.

[29] Sonawane, M. R.; Nagare, B. J.; Habale, D.; Shivade, R. K., Comparative study of adsorption of O_2, CO_2, NO_2 and SO_2 on pristine and Si-doped carbon nanotubes. *Adv. Mate. Res.* **2013**, *678*, 179-184, DOI: 10.4028/www.scientific.net/AMR.678.179.

[30] Ghasemi, A. S.; Rezaei, M.; Molla, M., Density functional theory (DFT) study adsorptions on single-walled carbon nanotube-a review. *Int. J. Chem. Tech. Res.* **2013**, *5*, 1594-1601.

[31] Mirzaei, M.; Kalhor, H. R.; Hadipour, N. L., Covalent hybridization of CNT by thymine and uracil: A computational study. *J. Mol. Model*. **2011**, *17*, 695-699, DOI: 10.1007/s00894-010-0771-z. Epub 2010 Jun 8.

[32] Zhang, X.; Dai, Z.; Wei, L.; Liang, N.; Wu, X., Theoretical calculation of the gas-sensing properties of Pt-decorated carbon nanotubes. *J. Sensors*. **2013**, *13*, 15159-15171, DOI: 10.3390/s131115159.

[33] Pabitra, N. S.; Kalyan, K., Das, Adsorption sensitivity of zigzag GeC nanotube towards N_2, CO, SO_2, HCN, NH_3, and H_2CO molecules. Chem. Phys. Lett. **2013**, *577*, 107-113, DOI: 10.1016/j.cplett.2013.05.055.

[34] Yu, G. S.; Yi, W., Single-walled carbon nanotubes as a chemical sensor for so_2 detection. IEEE Trens. *Nanotechnol*. **2007**, *6*, 545-548, DOI: 10.1109/TNANO.2007.903800.

[35] Goldoni, A.; Larciprete, R.; Petaccia. L.; Lizzit, S., Single-wall carbon nanotube interaction with gases: sample contaminants and environmental monitoring. *J. Am. Chem. Soc.* **2003**, *125*, 11329-11333, DOI: 10.1021/ja034898e.

[36] Ao, Z. M.; Peeters, F. M., Electric field activated hydrogen dissociative adsorption to nitrogen-doped graphene. *J. Phys. Chem. C.* **2010**, *114*, 14503-14509, DOI: 10.1021/jp103835k.

[37] Zhou, J.; Wang, Q.; Sun, Q.; Jena, P.; Chen, X. S., Electric field enhanced hydrogen storage on polarizable materials substrates. *Proc. Natl. Acad. Sci.* **2010**, *107*, 2801-2806, DOI: 10.1073/pnas.0905571107.

[38] Alfieri, G.; Kimoto, T., Engineering the band gap of SiC nanotubes with a transverse electric field. *Appl. Phys. Lett.* **2010**, *97*, 1-3. DOI: 10.1063/1.3469944.

[39] Jia, Y. B.; Zhuang. G. L.; Wang. J. G.; Electric field induced silicon carbide nanotubes: a promising gas sensor for detecting SO_2. *J. Phys. D: Appl. Phys*. **2012**, *45*, 1-8, DOI: 10.1088/0022-3727/45/6/065305.

[40] Izadyar, M.; Gholizadeh, M.; khavani, M.; Housaindokht, M. R., Quantum chemistry aspects of the solvent effects on 3,4-dimethyl-2,5-dihydrothiophen-1,1-dioxide pyrolysis reaction", *J. Phys. Chem. A.* **2013**, *117*, 2427-2433, DOI: 10.1021/jp312746y.

[41] Frisch, M. J.; Trucks, G. W.; Schlegel, H. B.; Scuseria, G. E.; Robb, M. A.; Cheeseman, J. R.; Scalmani, G.; Barone, V.; Mennucci, B.; Petersson, G. A.; Nakatsuji, H.; Caricato, M.; Li, X.; Hratchian, H. P.; Izmaylov, A. F.; Bloino, J.; Zheng, G.; Sonnenberg, J. L.; Hada, M.; Ehara, M.; Toyota, K.; Fukuda, R.; Hasegawa, J.; Ishida, M.; Nakajima, T.; Honda, Y.; Kitao, O.; Nakai, H.; Vreven, T.; Montgomery, J. A. J.r.; Peralta, J. E.; Ogliaro, F.; Bearpark, M.; Heyd, J. J.; Brothers, E.; Kudin, K. N.; Staroverov, V. N; Kobayashi, R.; Normand, J.; Raghavachari, K.; Rendell, A.; Burant, J. C.; Iyengar, S. S.; Tomasi, J.; Cossi, M.; Rega, N.; Millam., M. J.; Klene, M.; Knox, J. E.; Cross, J. B.; Bakken, V.; Adamo, C.; Jaramillo, J.; Gomperts, R.; Stratmann, R. E.; Yazyev, O.; Austin, A. J.; Cammi, R.; Pomelli, C.; Ochterski, J. W.; Martin, R. L.; Morokuma, K.; Zakrzewski, V. G.; Voth, G. A.; Salvador, P.; Dannenberg, J. J.; Dapprich, S.; Daniels, A. D.; Farkas, Ö.; Foresman, J. B.; Ortiz, J. V.; Cioslowski, J.; Fox, D. J., (2009) Gaussian 09 references., Inc.; Pittsburgh PA.

[42] Dennington, R.; Keith, T.; Millam, J., (2009) Gaussview, version 5. Semichem Inc.: Shawnee Mission, KS. [43] http://www.jcrystal.com/products/ wincnt/Nanotube. *Nanotube Modeler.* 2004, version 1.2.4.

[43] Koopmans, T., Over the allocation of wave functions and eigenvalues for the individual electrons one atom. *Physica.* **1934**, *1*, 104-113, DOI: 10.5897/ AJB2014.13671.

[44] Peng, C.; Ayala, P. Y.; Schlegel, H. B.; Frisch, M. J., Using redundant internal coordinates to optimize equilibrium geometries and transition states. *J. Comput. Chem.* **1996**, *17*, 760-767, DOI: 10.1002/(sici)1096-987x(19960115)17:1<49::aid-jcc5>3.0.co;2-0.